Relative light yield and temporal response of a stilbene-doped bibenzyl organic scintillator for neutron detection

J. A. Brown, B. L. Goldblum, L. A. Bernstein, D. L. Bleuel, N. M. Brickner, J. A. Caggiano, B. H. Daub, G. S. Kaufman, R. Hatarik, T. W. Phillips, S. A. Wender, K. van Bibber, J. Vujic, and N. P. Zaitseva

Citation: Journal of Applied Physics **115**, 193504 (2014); doi: 10.1063/1.4878238
View online: http://dx.doi.org/10.1063/1.4878238
View Table of Contents: http://scitation.aip.org/content/aip/journal/jap/115/19?ver=pdfcov
Published by the AIP Publishing

Relative light yield and temporal response of a stilbene-doped bibenzyl organic scintillator for neutron detection

J. A. Brown,[1] B. L. Goldblum,[1,a)] L. A. Bernstein,[2] D. L. Bleuel,[2] N. M. Brickner,[1] J. A. Caggiano,[2] B. H. Daub,[1] G. S. Kaufman,[1] R. Hatarik,[2] T. W. Phillips,[2] S. A. Wender,[3] K. van Bibber,[1] J. Vujic,[1] and N. P. Zaitseva[2]
[1]*Department of Nuclear Engineering, University of California, Berkeley, California 94720, USA*
[2]*Lawrence Livermore National Laboratory, Livermore, California 94551, USA*
[3]*Los Alamos National Laboratory, Los Alamos, New Mexico 87545, USA*

(Received 23 April 2014; accepted 5 May 2014; published online 15 May 2014)

The neutron time-of-flight (nTOF) diagnostics used to characterize implosions at the National Ignition Facility (NIF) has necessitated the development of novel scintillators that exhibit a rapid temporal response and high light yield. One such material, a bibenzyl-stilbene mixed single-crystal organic scintillator grown in a 99.5:0.5 ratio in solution, has become the standard scintillator used for nTOF diagnostics at NIF. The prompt fluorescence lifetime and relative light yield as a function of proton energy were determined to calibrate this material as a neutron detector. The temporal evolution of the intensity of the prompt fluorescent response was modeled using first-order reaction kinetics and the prompt fluorescence decay constant was determined to be 2.46 ± 0.01 (fit) ± 0.13 (systematic) ns. The relative response of the bibenzyl-stilbene mixed crystal generated by recoiling protons was measured, and results were analyzed using Birks' relation to quantify the non-radiative quenching of excitation energy in the scintillator. © *2014 AIP Publishing LLC*. [http://dx.doi.org/10.1063/1.4878238]

I. INTRODUCTION

The National Ignition Facility (NIF) is a 192-beam, 1.9 MJ laser system designed to achieve ignition via inertial confinement fusion (ICF).[1] The lasers enter a target chamber through laser beam ports and are either focused directly on a deuterium-tritium-loaded capsule, or indirectly on the interior surface of a surrounding holhraum. The rapid ablation of the capsule surface leads to a complementary inward compression force that drives the capsule to temperature and density conditions conducive to ICF. The resulting spectrum of neutrons from thermonuclear reactions, including most notably 14.1 MeV neutrons from the D-T fusion reaction, is characterized using a large suite of neutron diagnostics. These include, among others, neutron activation diagnostics,[2] a magnetic recoil spectrometer,[3] and an array of neutron time-of-flight (nTOF) spectrometers.[4] The resulting data are employed to diagnose implosion performance by providing insight into neutron yield and ion temperature.

One of the most important quantities obtained using nTOF is the down-scattered ratio (DSR) of neutrons with energies between 10 and 12 MeV to unscattered 14.1 MeV neutrons. This ratio, which corresponds to the fraction of neutrons that have scattered a single time off of nuclei in the D-T fuel, is used as the primary indicator of peak fuel areal density (ρR_{fuel}). Measurements of the DSR using nTOF at NIF are particularly challenging in that the highest neutron flux (as high as $\sim 10^{17}$ 14.1 MeV neutrons/cm^2/s for a detector located 20 m from the center of the target chamber) arrives at the detector before the lower energy neutrons. This places a stringent requirement on nTOF detection systems that the light output as a function of time for the detector drop dramatically in a very short time period. A new class of single-crystal stilbene-doped bibenzyl organic scintillators was developed in order to accomplish this goal. The bibenzyl crystal was grown with 0.5% stilbene in solution to suppress the delayed fluorescence component of the scintillation light while maintaining an enhanced light yield.[5] This work details the measured scintillation properties of this mixed single-crystal organic scintillator. Section II consists of a description of the experimental layout and electronics configuration. In Sec. III, the methodology for characterization of the time evolution of the light emission pathways, determination of the neutron kinetic energy using nTOF, and the light output response for protons originating from neutron-proton scattering in the scintillator is established. Results on the prompt fluorescence lifetime and relative light yield of the stilbene-doped bibenzyl scintillator are discussed in Sec. IV. Concluding remarks are given in Sec. V.

II. EXPERIMENTAL CONFIGURATION

The 0.5% stilbene-doped bibenzyl mixed single-crystal organic scintillator was solution grown and cut to a size of $5.1 \times 5.7 \times 0.5$ cm^3. A $^2H^+$ beam from the 88-in. Cyclotron at Lawrence Berkeley National Laboratory (LBNL) was employed to generate neutrons in the experiment. A Faraday Cup, housing a 3.8 cm thick tantalum target, located in the cyclotron vault was used for both online beam monitoring and to produce "breakup" neutrons via the ^{nat}Ta(^{2}H,n) reaction. The neutron beam was collimated using a beam pipe encased in 3 m of concrete and 1.5 m of sandbags, resulting in a 10-cm-radius open-air neutron beam in the experimental area.

Time correlated single photon counting (TCSPC) was employed to characterize the scintillator light decay.[6] The crystal was mounted in an aluminum housing on the front

a)Electronic mail: bethany@nuc.berkeley.edu

face of a Hamamatsu H2431-50 photomultiplier tube (PMT) negatively biased to 1.4 kV in tandem with a Hamamatsu H5784-01 PMT loosely coupled via a 100 μm fiber optic cable with an input voltage of 12 V and a reference voltage of 0.9 V. The timing of output signals was established using constant fraction discriminator (CFD) modules produced by LBNL. The output signals from the CFD modules were fed into a CAEN V1290N multi-hit time-to-digital converter (TDC) operating in trigger matching mode with the clock multiplier of the module set to obtain 200 ps resolution. The master trigger was a time-delayed logic pulse from the closely coupled PMT. Data were acquired for a period of 2.2 h using a 29 MeV deuteron beam with a beam intensity of approximately 100 nA.

The measurement of the relative response of the scintillator utilized neutrons produced by a 16 MeV $^2H^+$ beam and a Hamamatsu H2431-50 PMT located 7.8 m downstream from the breakup target. The output signal was split with the timing chain as described above. Pulse height data were obtained using a mesytec MPD-4 module as a fast variable gain input amplifier fed to a CAEN V785 peak sensing analog-to-digital converter (ADC). The timing of the RF signal from the 88-in. Cyclotron converted to standard logic pulses using the CFD module was also recorded using the TDC. Data were acquired for a duration of 4.0 h with a beam intensity of approximately 200 nA, and recorded using the MIDAS data acquisition system.[7] Data reduction was performed using the ROOT data analysis framework.[8]

III. METHODOLOGY

A. Scintillation mechanisms and temporal response

Fast neutrons with energies below 29 MeV primarily deposit energy in an organic scintillator through the (n, p) scattering reaction. The recoiling protons transfer energy to the system through excitation and ionization of the organic molecules. The electronic excitations populate singlet states, and rapid de-excitations from the excited singlet-state band result in prompt fluorescence. Intersystem crossing leads to the population of the triplet-state band. The triplet-to-singlet de-excitation tends to occur over longer time scales and results in phosphorescent light emission. These triplet excitons are mobile, and when close in space, triplet-triplet annihilation can occur leaving one of the electrons in the singlet ground-state band and the other in the singlet excited-state band. The resulting radiative de-excitation from the singlet excited states, termed delayed fluorescence, is rate-limited based on nearest-neighbor triplet-triplet annihilation and long-range triplet exciton migration and annihilation.[9]

The singlet and triplet state population densities, n_S and n_T, respectively, can be described via the following coupled set of differential equations:

$$\frac{dn_S}{dt} = -K_S n_S - K_{ST} n_S + \phi K_{TT} n_T^2, \tag{1}$$

and

$$\frac{dn_T}{dt} = K_{ST} n_S - K_T n_T - K_{TT} n_T^2, \tag{2}$$

where K_S, K_T, K_{TT}, and K_{ST} are the rate constants for monomolecular singlet decay (prompt fluorescence), monomolecular triplet decay (phosphorescence), triplet-triplet annihilation, and radiationless singlet-triplet transition (intersystem crossing), respectively. The ϕ term represents the fraction of excited singlet states populated via triplet-triplet annihilation and is $\leq \frac{1}{2}$. This treatment assumes an instantaneous population of the excited singlet states[10] and that contributions due to radiationless singlet-singlet transitions are negligible.

For the bibenzyl-stilbene (99.5:0.5) mixed single-crystal scintillator, the stilbene dopant acts as a trap for the triplet excitations of the bibenzyl host molecule.[5] At low concentrations, this strongly limits triplet-triplet interactions. As such, $K_{TT} \approx 0$. Further, the internal spin-orbit coupling rate is low (i.e., $K_{ST} \ll K_S$), allowing Eq. (1) to be rewritten as

$$\frac{dn_S}{dt} = -K_S n_S, \tag{3}$$

or

$$n_S(t) = \alpha e^{-\frac{t}{\tau}}, \tag{4}$$

where $\tau = 1/K_S$ is the mean prompt fluorescence lifetime and α is the initial population of the excited singlet states.

To describe the measured intensity of the light emission as a function of time, $I(t)$, the time-dependent singlet state population density is convolved with a Gaussian distribution representative of the intrinsic temporal response of the detection system. Based on first-order reaction kinetics, the measured intensity of the light emission as a function of time is directly proportional to $n_S(t)$ and is given by

$$\begin{aligned} I(t) &= \int_0^\infty e^{-\frac{1}{2}\left(\frac{t}{\sigma}\right)^2} \alpha e^{-\frac{t}{\tau}} dt \\ &= \alpha e^{\left(\frac{\sigma^2}{2\tau^2} - \frac{t}{\tau}\right)} \left[1 + \operatorname{erf}\left(\frac{t}{\sqrt{2}\sigma} - \frac{\sigma}{\sqrt{2}\tau}\right)\right] + B, \end{aligned} \tag{5}$$

where σ is the standard deviation of the Gaussian distribution and B is a constant background term representative of random coincidences.

B. Neutron time-of-flight

Using the neutron time-of-flight method, the relativistic time-energy relationship is employed to determine the kinetic energy of incident neutron

$$E = (\gamma - 1) m_n c^2, \tag{6}$$

where

$$\gamma = \frac{1}{\sqrt{1 - \frac{(x/t)^2}{c^2}}}. \tag{7}$$

Here, m_n is the rest mass of the neutron, c is the speed of light, x is the neutron flight path (i.e., distance between the

breakup target and the detector), and t is the time-of-flight of the neutron. Using the γ ray production originating from the interaction of the charged primary beam in the breakup target as a fiducial marker, an absolute reference to the time of neutron production was obtained.

C. Scintillation response

The scintillation light output for organic scintillators is well described using Birks relation[11]

$$\frac{dL}{dx} = \frac{S(dE/dx)}{1 + kB(dE/dx)}, \tag{8}$$

where dL/dx is the energy-dependent scintillation light yield per unit path length, dE/dx is the energy-dependent stopping power, or energy deposited per unit path length, S is the scintillation efficiency, k is a quenching parameter (i.e., the fraction of the primary excitation that undergoes radiationless deexcitation), and B is Birks constant. Equation (8) can be written in the form

$$\frac{dL}{dE} = \frac{S}{1 + kB(dE/dx)}, \tag{9}$$

where dL/dE is the scintillation light yield per unit energy loss. The product kB, termed Birks parameter, is an experimentally determined constant dependent upon the scintillation medium. Birks' parameter is used to quantify the proton light yield and is an important input for Monte Carlo simulations of the scintillation response for neutrons.

IV. RESULTS AND DISCUSSION

Figure 1 shows the time dependence of the scintillation light from the 0.5% stilbene-doped bibenzyl scintillator obtained using TCSPC. Photon contributions were removed using time-of-flight gating to isolate the neutron response. The data were fit using Eq. (5), denoted by the dashed line in Fig. 1, via the Minuit MIGRAD function minimization routine.[12] The uncertainty in the fit parameters were obtained using MINOS error analysis methods[13] with a χ^2 per degrees of freedom of 1.17. The σ parameter, representative of the uncertainty in the measurement of temporal differences, was determined to be 0.47 ± 0.01 ns, and is dominated by the inherent resolution of the electronic components of the data acquisition system. The prompt fluorescence decay constant was determined to be 2.46 ± 0.01 (fit) ± 0.13 (systematic) ns. To quantify the systematic uncertainty, the fit range was varied, and the maximum variation was taken as symmetric systematic uncertainty. This result is consistent with previous measurements of the primary light decay constant.[14]

The small concentration of stilbene impurity traps in this mixed crystal suppresses the rates of nearest neighbor triplet-triplet annihilation and long-range triplet exciton migration and annihilation. This results in a dramatic suppression of the delayed fluorescence component of the scintillation light as compared to that for higher stilbene dopant ratios. Approximately, 95% of the total light yield was collected in 9.5 ns. The rapid prompt fluorescent and highly suppressed delayed fluorescent mechanisms make this material useful for nTOF experiments with high neutron flux.

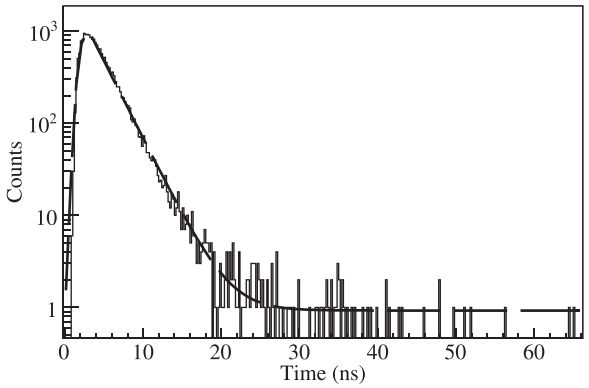

FIG. 1. Time dependence of intensity of scintillation light from a 0.5% stilbene-doped bibenzyl mixed single-crystal organic scintillator. The dashed line represents a fit to the data using a single component exponential decay convolved with a Gaussian distribution.

Calculations of the relative light yield of the 0.5% stilbene-doped bibenzyl scintillator as a function of neutron energy require input data on the light output of the scintillator for various particle types as a function of particle energy.[15] While reactions on carbon represent an increasingly important contribution to the light yield for neutrons with energies greater than ~20 MeV, neutron elastic scattering on protons represents the dominant mechanism for light production in organic scintillators for fast neutrons. To obtain the relative response of the 0.5% stilbene-doped bibenzyl mixed single-crystal organic scintillator as a function of proton energy deposited, a two-dimensional histogram of pulse height versus nTOF was generated. The data were binned in time intervals of 4 ns, representative of the full width at half maximum (FWHM) of the photon signal, and transformed into the energy domain as described in Eq. (6). The resulting two-dimensional histogram of pulse height versus neutron energy is shown in Fig. 2.

The pulse height spectrum for each energy bin was fit using a complementary error function

$$\phi(x) = a_0 \,\mathrm{erfc}\left(\frac{x - \phi_0}{a_1}\right) = \frac{2}{\pi}\int_x^{\inf} C_0 H(\phi_0 - x) e^{-\left(\frac{x-y}{a_1}\right)^2} dy. \tag{10}$$

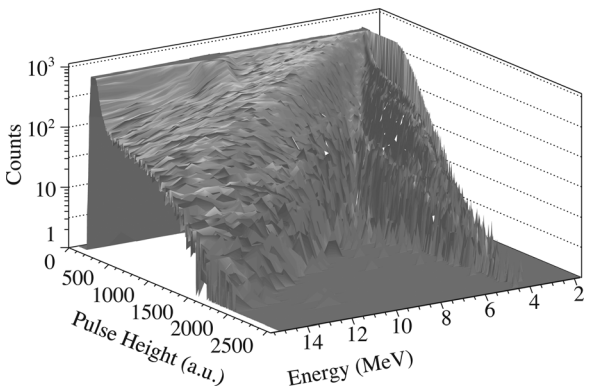

FIG. 2. Two-dimensional surface plot of pulse height in arbitrary units versus neutron energy in MeV. The ridge at 4 MeV corresponds to high energy neutrons produced from the following cyclotron beam pulse.

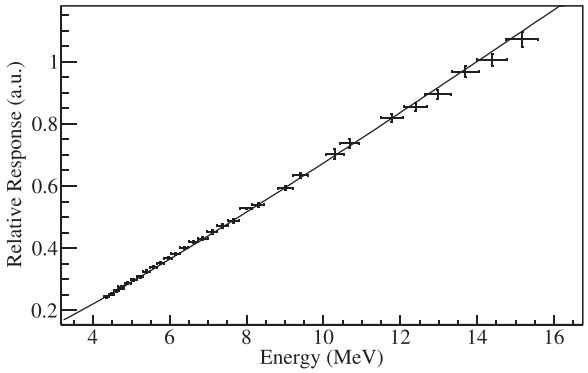

FIG. 3. The data points represent the relative light yield of the 0.5% stilbene-doped bibenzyl mixed single-crystal organic scintillator as a function of proton energy deposited in MeV. The energy bin width varies via a non-linear transformation using 4 ns time bins. The line represents a fit to the data using Birks' semi-empirical relation for the number of scintillation photons generated as a function of proton energy deposited.

The complementary error function describing the pulse height spectrum, $\phi(x)$, where x is the pulse height in arbitrary units, is representative of the convolution of a Heaviside step function with a Gaussian spreading function, where a_0 is a normalization constant corresponding to the height of the pulse height spectrum, ϕ_0 is the value corresponding to the position of the edge of the Heaviside step function in pulse height units, and a_1 is related to the FWHM of the Gaussian function. The pulse height corresponding to the maximum hydrogen recoil energy for each bin, x_{max}, was determined using the pulse height at which the spectrum was at 1% of the maximum value, a_0 [i.e., $\phi(x_{max}) = 0.001a_0$]. To ensure that the edge of the pulse height distribution corresponded to maximum proton energy deposition, the range of protons at the maximum incident neutron energy was calculated using the energy loss and straggling tool (ELAST).[16] The range corresponding to 16 MeV protons in bibenzyl is 2.9 mm and thus, edge effects in the determination of x_{max} were assumed to be negligible. The uncertainty in x_{max} was obtained by summing in quadrature the parameter estimation errors provided by the MINOS minimization routine.

Using this prescription, a plot of the relative response of the stilbene-doped bibenzyl mixed single-crystal organic scintillator as a function of proton energy deposited was obtained as shown in Fig. 3. To determine Birks' parameter, the stopping power for protons in bibenzyl was calculated using ELAST as a function of proton energy. Using discretized values of the stopping power, Eq. (9) was energy-integrated to obtain $L(E)$, and a χ^2-minimization was performed between this function and the measured relative response data using the Minuit MIGRAD function minimization routine. The kB parameter for the bibenzyl-stilbene (99.5:0.5) mixed single-crystal scintillator was determined to be 3.862 ± 0.795 mg/(MeV cm^2). This value is similar to the measured kB values for other organic scintillators.[17]

V. CONCLUSION

The bibenzyl-stilbene (99.5:0.5) mixed single-crystal scintillator exhibits rapid prompt fluorescence and highly suppressed delayed fluorescence light emission mechanisms, making it a good candidate for high-event-rate pulse mode operation and current-mode nTOF measurements at NIF and other energetic ICF devices, where signals that differ by orders of magnitude occurring within hundreds of nanoseconds must be differentiated. The prompt fluorescence decay constant was determined and compared favorably to previous measurements. The relative light yield as a function of proton energy deposited was obtained, and Birks' parameter was extracted, which can be used as input to simulations to determine the nTOF instrument response function for the bibenzyl-stilbene mixed single-crystal organic scintillator. Future work includes utilization of an electrostatic deflector at the 88-in. Cyclotron at Lawrence Berkeley National Laboratory to obtain a direct measurement of the neutron response of this scintillator over a broader energy range relevant for nTOF diagnostics.

ACKNOWLEDGMENTS

The authors would like to thank the 88-in. Cyclotron operations and facilities staff for their help in performing this experiment. This work was performed under the auspices of the U.S. Department of Energy by Lawrence Livermore National Laboratory under Contract No. DE-AC52-07NA27344, Lawrence Berkeley National Laboratory under Contract No. DE-AC02-05CH11231, the National Nuclear Security Administration under Award No. DE-NA0000979, The Nuclear Science and Security Consortium, and the University of California Office of the President Laboratory Fees Research Program under Award No. 12-LR-238745.

[1]G. H. Miller, E. I. Moses, and C. R. Wuest, Nucl. Fusion **44**, S228 (2004).
[2]D. L. Bleuel, C. B. Yeamans, L. A. Bernstein, R. M. Bionta, J. A. Caggiano, D. T. Casey, G. W. Cooper, O. B. Drury, J. A. Frenje, C. A. Hagmann, R. Hatarik, J. P. Knauer, M. G. Johnson, K. M. Knittel, R. J. Leeper, J. M. McNaney, M. Moran, C. L. Ruiz, and D. H. G. Schneider, Rev. Sci. Instrum. **83**, 10D313 (2012).
[3]J. A. Frenje, D. T. Casey, C. K. Li, F. H. Séguin, R. D. Petrasso, V. Y. Glebov, P. B. Radha, T. C. Sangster, D. D. Meyerhofer, S. P. Hatchett, S. W. Haan, C. J. Cerjan, O. L. Landen, K. A. Fletcher, and R. J. Leeper, Phys. Plasmas **17**, 056311 (2010).
[4]V. Y. Glebov, T. C. Sangster, C. Stoeckl, J. P. Knauer, W. Theobald, K. L. Marshall, M. J. Shoup, T. Buczek, M. Cruz, T. Duffy, M. Romanofsky, M. Fox, A. Pruyne, M. J. Moran, R. A. Lerche, J. McNaney, J. D. Kilkenny, M. J. Eckart, D. Schneider, D. Munro, W. Stoeffl, R. Zacharias, J. J. Haslam, T. Clancy, M. Yeoman, D. Warwas, C. J. Horsfield, J.-L. Bourgade, O. Landoas, L. Disdier, G. A. Chandler, and R. J. Leeper, Rev. Sci. Instrum. **81**, 10D325 (2010).
[5]N. Zaitseva, A. Glenn, L. Carman, R. Hatarik, S. Hamel, M. Faust, B. Schabes, N. Cherepy, and S. Payne, IEEE Trans. Nucl. Sci. **58**, 3411 (2011).
[6]L. M. Bollinger and G. E. Thomas, Rev. Sci. Instrum. **32**, 1044 (1961).
[7]See http://midas.triumf.ca for "MIDAS Data Acquisition Software Package."
[8]R. Brun and F. Rademakers, Nucl. Instrum. Methods Phys. Res., Sect. A **389**, 81 (1997).
[9]H. Sternlicht, G. C. Nieman, and G. W. Robinson, J. Chem. Phys. **38**, 1326 (1963).
[10]L. Papadopoulos, Nucl. Instrum. Methods Phys. Res., Sect. A **401**, 322 (1997).
[11]J. B. Birks, Proc. Phys. Soc. A **64**, 874 (1951).
[12]F. James, *MINUIT Function Minimization and Error Analysis Reference Manual*, CERN Program Library Long Writeup D506, version 94.1 (CERN, Geneva, Switzerland, 1998).

[13]W. T. Eadie, D. Drijard, F. James, M. Roos, and B. Sadoulet, *Statistical Methods in Experimental Physics* (North-Holland Pub. Co., 1971).
[14]R. Hatarik, L. A. Bernstein, J. A. Caggiano, M. L. Carman, D. H. G. Schneider, N. P. Zaitseva, and M. Wiedeking, Rev. Sci. Instrum. **83**, 10D911 (2012).
[15]N. R. Stanton, C00-1545-92, 1971.
[16]"Energy loss and Straggling Tool," [Adapted from the computer program ENELOSS, written by H. Ernst (1981) with stopping power routines by K. Lesko (1984)].
[17]R. L. Craun and D. L. Smith, Nucl. Instrum. Methods **80**, 239 (1970).